HHS Public Access

Author manuscript

J Am Chem Soc. Author manuscript; available in PMC 2019 October 31.

Published in final edited form as:

J Am Chem Soc. 2019 July 31; 141(30): 11892–11904. doi:10.1021/jacs.9b02893.

Energy Decomposition Analyses Reveal the Origins of Catalyst and Nucleophile Effects on Regioselectivity in Nucleopalladation of Alkenes

Xiaotian Qi[†], **Daniel G. Kohler**[‡], **Kami L. Hull**[‡,*], **Peng Liu**[†,§,*]

[†]Department of Chemistry, University of Pittsburgh, Pittsburgh, PA 15260, USA

[‡]Department of Chemistry, University of Texas at Austin, Austin, TX 78712, USA.

[§]Department of Chemical and Petroleum Engineering, University of Pittsburgh, Pittsburgh, PA 15261, USA

Abstract

Nucleopalladation is one of the most common mechanisms for Pd-catalyzed hydro- and oxidative functionalization of alkenes. Due to the electronic bias of the π-alkene-palladium complexes, nucleopalladations with terminal aliphatic alkenes typically deliver the nucleophile to the more substituted sp_2 carbon to form the Markovnikov-selective products. The selective formation of the *anti*-Markovnikov nucleopalladation products requires the inherent electronic effects to be overridden, which is still a significant challenge for reactions with simple aliphatic alkenes. Because the interactions between the nucleophile and the alkene substrate are influenced by a complex combination of multiple types of steric and electronic effects, a thorough understanding of the interplay of these underlying interactions is needed to rationalize and predict the regioselectivity. Here, we employ an energy decomposition approach to quantitatively separate the different types of nucleophile-substrate interactions, including steric, electrostatic, orbital interactions, and dispersion effects, and to predict the impacts of each factor on regioselectivity. We demonstrate the use of this approach on the origins of catalyst-controlled *anti*-Markovnikov-selectivity in Hull's Pd-catalyzed oxidative amination reactions. In addition, we evaluated the regioselectivity in a series of nucleopalladation reactions with different neutral and anionic Pd catalysts and *N*- and *O*-nucleophiles with different steric and electronic properties. Based on these computational analyses, a generalized scheme is established to identify the dominant nucleophile-substrate interaction affecting the regioselectivity of nucleopalladations with different Pd catalysts and nucleophiles.

INTRODUCTION

Palladium-catalyzed hydro- and oxidative functionalization of unactivated aliphatic alkenes is an efficient and atom-economical synthetic strategy for new C−C and C−heteroatom bond

[*]**Corresponding Author** kamihull@utexas.edu, pengliu@pitt.edu.

Supporting Information. Additional discussions of computational results, Cartesian coordinates, and energies of all computed structures are included in the Supporting Information. This material is available free of charge via the Internet at http://pubs.acs.org.

The authors declare no competing financial interest.

formation.[1] One of the most common mechanistic pathways in these reactions involve nucleopalladation, in which a nucleophilic coupling partner attacks a π-alkene-Pd complex via either *syn*-insertion or *anti*-attack (also referred to as *cis*- and *trans*-nucleopalladation, respectively).[2] Controlling the regioselectivity still remains a significant challenge in intermolecular nucleopalladation with sterically and electronically unbiased aliphatic alkenes.[3] Most nucleopalladation reactions favor the Markovnikov products, in which the nucleophile is added to the more substituted carbon of the alkene. Although a broad variety of *N*- and *O*-nucleophiles have been employed in nucleopalladations,[4] examples that override the intrinsic Markovnikovselectivity are rare. A practical challenge in the rational design of catalyst-controlled *anti*-Markovnikov selective reactions is that the dominant factor controlling the regioselectivity remains ambiguous. A sensible explanation to the regioselectivity control is based on favored electrostatic interactions between the nucleophile and the more substituted internal sp_2-carbon to provide the Markovnikov addition products (Figure 1a). In addition, orbital interactions,[5] steric,[4a,6] and dispersion[7] effects are also expected to impact the regioselectivity (Figure 1b). Therefore, a thorough understanding of how the different types of effects contribute to the regioselectivity, and more importantly, how the individual factors can be fine-tuned, is essential for the development of *anti*-Markovnikov selective transformations that overcome the inherent electronic preferences.

Dissecting the multiple underlying effects and rationalizing the major factors for the regioselectivity control is also challenging in computational studies. A number of computational studies have been reported for functionalization of aliphatic alkenes via migratory insertion mechanisms, in which steric effects typically dominate the regioselectivity.[8] In contrast, computational studies on the regioselective nucleopalladation of alkenes are limited due to the complexity of regioselectivity control.[9] The potential competition between *cis*- and *trans*-nucleopalladation pathways[1c,10] further complicated the computational analysis (Figure 1a). Here, we present a systematic computational approach to quantitatively analyze the contributions of different types of effects to the regioselectivity in *cis*- and *trans*-nucleopalladations with different palladium catalysts and a variety of *N*- and *O*-nucleophiles with different formal charges, steric hinderances, and nucleophilicities (Figure 1c). Using the distortion-interaction/activation-strain model[11] and energy decomposition analysis (EDA)[12] methods, the computed regioselectivity is dissected into steric repulsions, electrostatic interactions, orbital interactions, and dispersion interactions between the nucleophile and the substrate. This decomposition approach allows for a straightforward way to reveal the dominant factor for regioselectivity control. Therefore, the origin of regioselectivity in different catalyst systems and in reactions with different nucleophiles can be rationally predicted.

Here, we report the use of this energy decomposition approach to study the origin of the catalyst-controlled *anti*-Markovnikov regioselectivity in the Pd-catalyzed oxidative amination of terminal alkenes, developed by the Hull group.[13] In this reaction, the addition of Bu_4NCl and Bu_4NOAc effectively reverses the regioselectivity to favor the *anti*-Markovnikov amination products (Figure 2a). This is a unique example where complete regioselectivity reversal is achieved by simply changing the neutral $Pd(OAc)_2$ catalyst[4d] system to a putative anionic Pd catalyst.[14] Previously, the Hull group performed detailed mechanistic investigations using selectively deuterium labeled substrates and revealed

important mechanistic insights into the C–N bond formation (Figure 2b).[13] In the first experiment (eq. 1), 2,2-dideuterohomoallyl benzene was subjected to the reaction conditions; the selective migration of one deuterium to C3 and the second deuterium being at both C2 and C1 is consistent with the reaction occurring via aminopalladation (**TS-III** or **TS-IV**, Figure 1a) and eliminates the possibility of an allylic C–H activation. The second experiment (eq. 2), obtaining the monodeuteron product from the reaction with (*Z*)-2-deuterostyrene supports that the reaction is occurring through a *trans*aminopalladation via **TS-IV** rather than *cis*-aminopalladation via **TS-III** (Figure 1a). In addition, kinetic experiments suggested that an associative ligand exchange of Cl– or OAc– for an olefin is the turnover-limiting step (TLS) and that monomeric [Pd] is the resting state, but that both monomeric and dimeric Pd complexes are active catalysts. While this is key information about the catalytic cycle, it limits the experimental investigations that can be conducted to investigate the *anti*-Markovnikov selectivity as the C–N bond formation occurs after the TLS. The catalyst-controlled regioselectivity may be resulting from a few possible effects. First, the additives may change the number of available coordination sites on the Pd,[10b,15] which will affect the preferred mechanism for aminopalladation. The additional anionic ligand may block the coordination site on the Pd and prevent nucleophile coordination in the *cis*aminopalladation. Second, the electronic property of the Pd catalyst should affect the partial atomic charges, molecular orbital energies and coefficients of the alkene.[16] Therefore, both electrostatics and orbital interactions between the alkene and the nucleophile are expected to be different with the neutral and the anionic palladium catalysts. Lastly, the catalyst may also affect the forming C–N bond distances in the transition states, which could affect the sensitivity to the steric repulsions and/or London dispersion interactions between the nucleophile and the alkene. Here, we demonstrate the energy decomposition approach can quantitatively dissect the contributions from different factors in both *cis*- and *trans*aminopalladation with different Pd catalysts. While the regioselectivity is always affected by multiple factors, the computational analysis provided a straightforward way to predict which factor is dominant in each nucleopalladation reaction. We expect these chemically meaningful insights into the origin of catalyst and nucleophiles effects on the regioselectivity can be utilized to facilitate the catalyst design of regioselective and regiodivergent alkene functionalization reactions.

COMPUTATIONAL METHODS

Geometry optimizations and single-point energy calculations were carried out using Gaussian 09.[17] The geometries of intermediates and transition states were optimized using the B3LYP functional[18] with a mixed basis set of SDD for Pd and 6–31+G(d) for other atoms in the gas phase. Vibrational frequency calculations were performed for all the stationary points to confirm if each optimized structure is a local minimum or a transition state structure. Truhlar's quasi-harmonic corrections[19] were applied for entropy calculations using 100 cm^{-1} as the frequency cut-off. Solvation energy corrections and CHelpG atomic charges were calculated in dimethylacetamide (DMA) solvent with the SMD continuum solvation model[20] based on the gas-phase optimized geometries. The M06 functional[21] with a mixed basis set of SDD for Pd and 6–311+G(d,p) for other atoms was used for solvation single-point energy calculations. The energy decomposition analysis (EDA) calculations

were performed to dissect the computed gas-phase activation energy ($\Delta E‡$). In our decomposition approach, the activation energy is first separated into the distortion energy (ΔE_{dist}) of the two reactive fragments to reach their transition state geometries and the interaction energy (ΔE_{int}) between the two fragments using the following equation:[11a,11d]

$$\Delta E_{‡} = \Delta E_{dist} + \Delta E_{int}$$

For *cis*-aminopalladation transition states (**9M-TS** and **9A-TS**), the two fragments include the alkene and the $(AcO)^2$Pd–NPhth complex as the nucleophile. For *trans*-aminopalladation transition states (**6M-TS**, **6A-TS**, **12M-TS**, **12A-TS**), the two fragments include the Pd-alkene complex and the phthalimide anion or the diisopropylamine as the nucleophile. Using the second-generation energy decomposition analysis based on absolutely-localized molecular orbitals (ALMO-EDA)[22] in Q-Chem 5.0,[23] the interaction energy (ΔE_{int}) between the two fragments is dissected according to the following equation:

$$\Delta E_{int} = \Delta E_{Pauli} + \Delta E_{elstat} + \Delta E_{pol} + \Delta E_{ct} + \Delta E_{disp}$$

The ALMO-EDA calculations were performed at the M06/6–311G(d,p)−LANL2DZ level of theory. The dispersion term is computed using the second-generation ALMO-EDA by calculating the difference of the “frozen interaction” term from a standard exchange-correlation functional and from an auxiliary “dispersion free” exchange correlation functional.[22c,22d] HF is used as the “dispersion free” exchange correlation functional in the dispersion energy calculations.

Structures along the reaction coordinates in Figure 6 were obtained from intrinsic reaction coordinate (IRC) calculations. The Markovnikov and *anti*-Markovnikov transition states usually have different forming C–N bond distances. To minimize the effects of early or late transition states in comparing the differences of each energy term between the two regioisomeric pathways, the $\Delta\Delta E$ reported in all pie charts (Figures 7–9) were computed using the average of $\Delta\Delta E$ values at the two C–N bond distances that correspond to the Markovnikov and *anti*-Markovnikov transition states, respectively:

$$\begin{aligned}\Delta\Delta E_{ave} &= 1/2\ (\Delta\Delta E_{dis1} + \Delta\Delta E_{dis2}) \\ &= 1/2\ \left[\left(\Delta E_{M(dis1)} - \Delta E_{A(dis1)}\right) + \left(\Delta E_{M(dis2)} - \Delta E_{A(dis2)}\right)\right]\end{aligned}$$

Here, dis1 and dis2 are the forming C–N bond distances at the two regioisomeric transition states. ΔE_M and ΔE_A are the EDA energy terms at a given C–N bond distance along the Markovnikov and *anti*-Markovnikov reaction coordinates, respectively. The Complementary Occupied-Virtual Pairs (COVPs)[24] calculations were performed using Q-Chem 5.0 at the M06/6–311G(d,p) (LANL2DZ for Pd) level of theory. The ΔE_{ct} shown in Figure 7 is the charge transfer energy derived from the most significant COVPs. To be consistent with other EDA calculations, the ΔE_{ct}(COVP) values were calculated from the average of two structures with C–N bond constrained to dis1 and dis2, where dis1 and dis2 are the C–N bond distances at the two regioisomeric transition states:

$$\Delta E_{ct}(\text{COVP}) = 1/2 \left[\Delta E_{ct(dis1)}(\text{COVP}) + \Delta E_{ct(dis2)}(\text{COVP})\right]$$

The optimized structures and the COVP orbitals were visualized using CYLview[25] and GaussView 6.0.

RESULTS AND DISCUSSION

Mechanisms and Regioselectivity-Determining Step of the Pd-Catalyzed Oxidative Amination

Prior to applying the energy decomposition analysis to study the origin of regioselectivity, we needed to identify the regioselectivitydetermining step in the Pd-catalyzed oxidative amination reactions. Therefore, we computed the catalytic cycles of the oxidative amination of alkene **1** with both neutral and anionic palladium catalysts.[26] The DFT calculations indicated the aminopalladation is irreversible and is the regioselectivity-determining step.[27] The computed energy profiles of the neutral $Pd(OAc)_2$-catalyzed aminopalladation step of alkene **1** with phthalimide anion[28] are shown in Figure 3. The *anti*-Markovnikov and Markovnikov *trans*-aminopalladation of the p-alkene complex **5** (**6A-TS** and **6M-TS**) require 17.0 and 16.7 kcal/mol with respect to **5**, respectively. In the *cis*aminopalladation pathway, a stable anionic complex **8** is formed via the coordination of the phthalimide anion with the Pd center in complex **5**. Subsequent *anti*-Markovnikov and Markovnikov aminopalladations occur through four-membered cyclic transition states **9A-TS** and **9M-TS**, respectively. Both **9A-TS** and **9M-TS** are lower in energy than the *trans*-aminopalladation transition states **6A-TS** and **6M-TS**. This indicates the most favorable mechanism for the reaction with the neutral Pd catalyst is the *cis*aminopalladation. This conclusion is consistent with previous mechanistic studies that suggest reactions with strongly coordinating nucleophiles prefer the *cis*-nucleopalladation.[1c,10a]

In the presence of Bu_4NCl or Bu_4NOAc additives,[13] the anionic Cl- or OAc- ligand could coordinate to the neutral palladium catalyst to form palladate complexes.[10b,15] Because the chloride and acetate salts can both promote the *anti*-Markovnikov regioselectivity, we chose acetate additives in the calculations for simplicity (*i.e.* with $Pd(OAc)^3$ - as the active catalyst).[29] As shown in Figure 4, the formation of the palladate complex **10** through coordination of an acetate anion to the neutral $[Pd(OAc)_2]^3$ is slightly endergonic by 1.7 kcal/mol. Therefore, this equilibrium is expected to shift to favor the palladate complex at higher additive concentrations. From the palladate-alkene complex **11**, the *trans*-attack of the phthalimide anion requires 23.2 and 26.3 kcal/mol for *anti*-Markovnikov and Markovnikov additions (**12A-TS** and **12M-TS**), respectively. In contrast, the outer-sphere *cis*-aminopalladation, in which the nucleophile does not coordinate with the Pd center, requires much higher activation energies (See Figure S5 for details). The inner-sphere *cis*-aminopalladation requires one of the acetate ligands to be replaced by a phthalimide anion to form complex **8**. The *cis*-aminopalladation transition states from **8** are the same as those with the neutral $Pd(OAc)_2$ catalyst (**9A-TS** and **9MTS**, Figure 3). Therefore, this pathway would lead to the Markovnikov- selective products, rather than the *anti*-Markovnikov products observed experimentally under these conditions. Thus, this inner-sphere *cis*-

aminopalladation pathway is unlikely. Therefore, the most favorable mechanism with the anionic catalytic system is *trans*-aminopalladation, which is consistent with the deuterium labeling experiments by the Hull group.[13]

Taken together, the DFT calculations suggest the oxidative amination with the neutral Pd catalyst occurs via the *cis*aminopalladation mechanism,[4d] while the reaction with the anionic Pd catalyst occurs via the *trans*-aminopalladation mechanism. The aminopalladation is the regioselectivity-determining step. The computationally predicted regioselectivities in the aminopalladation with the neutral and anionic palladium catalysts agree well with the experimental observation (Figure 2a). With the neutral catalyst, the Markovnikov-selective *cis*-aminopalladation (**9M-TS**) is favored by 2.7 kcal/mol. The complete regioselectivity reversal is observed with the anionic catalyst, which strongly favors the *anti*-Markovnikov-selective *trans*-aminopalladation pathway (**12A-TS**) by 3.1 kcal/mol.[30]

The energy decomposition analysis approach to dissect the effects controlling the regioselectivity

Although the computational results nicely reproduced the experimental regioselectivity trend, it remains a challenge to provide a chemically meaningful explanation to the origin of the selectivity. As discussed in the Introduction, the reversal of regioselectivity may be due to several different effects. To establish a general understanding of the origin of regioselectivity, we performed energy decomposition analysis (EDA) calculations to study the oxidative amination reaction described above and a number of related nucleopalladation processes with different nucleophiles and Pd catalysts. Here, we first demonstrate the detailed steps of using the EDA approach to study the neutral $Pd(OAc)_2$-catalyzed C−N formation transition states with phthalimide anion (*i.e.* **9M-TS**, **9A-TS**, **6MTS**, and **6A-TS**). The same procedure is then applied to study other nucleopalladation reactions.

Equation 3 was used to dissect the contributions of different types of nucleophile-substrate interactions in the aminopalladation transition states (Figure 5). First, using the distortion/interaction model,[11] the activation energy of each transition state ($\Delta E‡$) is decomposed into distortion energy (ΔE_{dist}) of the two reactive fragments (highlighted in yellow and blue, respectively) and the interaction energy (ΔE_{int}) between these two fragments. Then, using the ALMO-EDA method,[22c] the interaction energy (ΔE_{int}) is further dissected into Pauli repulsion (ΔE_{Pauli}), electrostatic interactions (ΔE_{elstat}), polarization (ΔE_{pol}), charge transfer (ΔE_{ct}), and dispersion (ΔE_{disp}) (see Computational Methods for details). Specifically, ΔE_{elstat} is the Coulombic interactions between the two fragments, ΔE_{pol} is the stabilizing interactions from mixing of occupied and vacant orbitals within each fragment, and ΔE_{ct} is the interactions between an occupied orbital on one fragment and a vacant orbital on the other fragment. Among these terms, the sum of distortion energy (ΔE_{dist}) and Pauli repulsion (ΔE_{Pauli}) can be considered as the contribution of steric effects (ΔE_{steric}) to the overall activation energy. The sum of ΔE_{elstat}, ΔE_{pol}, and ΔE_{ct} describes electronic effects (ΔE_{elec}). Therefore, the overall activation energy ($\Delta E‡$) is dissected into contributions from steric effects (ΔE_{steric}), dispersion effects (ΔE_{disp}), and two different types of electronic effects, namely electrostatics (ΔE_{elstat}) and orbital interactions ($\Delta E_{orbital}$).[31]

Analysis of different types of nucleophile-substrate interactions along the reaction coordinate

We applied this EDA approach to study the four nucleopalladation pathways described in Figure 5. To analyze how the different types of nucleophile-substrate interactions vary along the nucleopalladation reaction coordinates, the computed energy terms with respect to the forming C–N (nucleophile) bond distances are illustrated in Figure 6. A few general conclusions about the origin of regioselectivity can be derived from the comparison of different pathways.

- Steric repulsions (ΔE_{steric}) are always less prominent in the *anti*-Markovnikov pathway (blue lines) than in the Markovnikov pathway (red lines). In contrast, both types of electronic effects (ΔE_{elstat} and $\Delta E_{orbital}$) always favor Markovnikov additions. Nucleophile-substrate dispersion interactions (ΔE_{disp}) also favor Markovnikov addition because dispersion interactions are larger when the nucleophile attacks the more substituted internal carbon of the alkene.
- While the different types of interactions are all stronger at shorter C–N distances, the vertical distances between the red and the blue lines ($\Delta\Delta E$) remain largely constant in the transition state region (2.0–2.3 Å). This indicates the energy difference between the Markovnikov and *anti*-Markovnikov pathways, *i.e.* contribution of each factor to the regioselectivity, is not affected by the location of the transition state along the reaction coordinate.
- The magnitude of each $\Delta\Delta E$ term can be very different among different reactions. For example, the difference of orbital interaction energies ($\Delta\Delta E_{orbital}$) is −17.1 kcal/mol in the four-membered cyclic *cis*-aminopalladation pathway (Figure 7a). This indicates the Markovnikov transition state **9M-TS** is strongly stabilized by orbital interactions. In contrast, the $\Delta\Delta E_{orbital}$ values are much smaller (*c.a.* −2~−4 kcal/mol) in the *trans*-aminopalladation pathways (Figure 7b), indicating much smaller effects of orbital interactions on regioselectivity in these reactions. Therefore, detailed analysis of the relative magnitudes of the different effects can reveal the dominant factor on regioselectivity in each reaction.

Identification of the dominant nucleophile-substrate interaction leading to the Markovnikov regioselectivity

The energy decomposition analysis results (Figure 6) are summarized as pie charts shown in Figure 7 to highlight the quantitative contributions of each type of nucleophile-substrate interactions to the overall regioselectivity in the aminopalladation with phthalimide anion. Each pie chart includes four different effects on regioselectivity. Among these, steric repulsions ($\Delta\Delta E_{steric}$) are the only effect that promotes *anti*-Markovnikov addition, while electrostatics ($\Delta\Delta E_{elstat}$), orbital interactions ($\Delta\Delta E_{orbital}$), and dispersions ($\Delta\Delta E_{orbital}$) promote Markovnikov addition. Therefore, because the sum of $\Delta\Delta E_{elstat}$, $\Delta\Delta E_{orbital}$, and $\Delta\Delta E_{disp}$ is greater than $\Delta\Delta E_{steric}$ in both *cis*- and *trans*-aminopalladation of **5**, the Markovnikov addition is preferred (Figure 7a and 7b). However, the dominant effects leading to the Markovnikov selectivity in these reactions are distinct from each other. In the

cis-aminopalladation (Figure 7a), the dominant effect that promotes the Markovnikov-selectivity (**9MTS**) is orbital interactions ($\Delta\Delta E_{orbital}$), while electrostatics ($\Delta\Delta E_{elstat}$) plays a more significant role in the *trans*-aminopalladation (**6MTS**, Figure 7b). On the other hand, dispersion effects are typically small compared with steric and electronic effects. This EDA analysis provides an unbiased and straightforward way to identify the dominant factor on regioselectivity. Therefore, a more in-depth theoretical investigation on the dominant effect can then be performed to provide additional mechanistic insights. To understand why orbital interactions promote Markovnikov selectivity in *cis*aminopalladation, we performed the Complementary Occupied-Virtual Pairs (COVPs) analysis[24] to study the donor-acceptor interactions between the Pd–Nu fragment and the alkene in the *cis*aminopalladation transition states (Figure 7a).[32] The COVP results revealed that the charge transfer between the occupied alkene π orbital and the vacant metal *d* orbital is the most important orbital interaction for the Markovnikov regioselectivity. This π→d orbital interaction is much more pronounced in the Markovnikov transition state **9M-TS** than in the *anti*-Markovnikov transition state **9ATS** ($\Delta E_{ct(\pi\rightarrow d)}$ = −41.9 and −33.1 kcal/mol, respectively). This is a result of the polarization of the occupied π orbital of the terminal aliphatic alkene (Figure 7a).[33] The FMO interactions between the HOMO of Pd-Nu and the π* of the alkene are comparable in the Markovnikov and *anti*-Markovnikov pathways ($\Delta E_{ct(\text{Pd-Nu}\rightarrow\pi^*)}$ = −21.1 and −19.8 kcal/mol in **9M-TS** and **9A-TS**, respectively). Therefore, the HOMO(Pd-Nu)/π* interactions have a smaller contribution to the regioselectivity (see Figure S10 for details). On the other hand, the dominant role of electrostatics ($\Delta\Delta E_{elstat}$) in $Pd(OAc)_2$-catalyzed Markovnikov-selective *trans*-aminopalladation is evidenced by the calculated CHelpG atomic charge on alkenes (Figure 7b).[34] Upon coordination with the $Pd(OAc)_2$ catalyst, the electron density on the C=C double bond becomes more polarized than in the free alkene with a greater amount of partial positive charge residing on the internal carbon.[35]

Effects of different *N*- and *O*-nucleophiles on regioselectivity

We then employed the EDA approach to study the origin of regioselectivity in nucleopalladation of the π-alkene/$Pd(OAc)_2$ complex **5** with a variety of *N*- and *O*-nucleophiles bearing different steric hindrances and formal charges. We surmised these investigations would reveal how the steric and electronic properties of the nucleophile affect the different types of nucleophile-substrate interactions. In addition, the differences between neutral and anionic nucleophiles, and between *N*- and *O*-nucleophiles are also explored. In agreement with previous experimental observations,[1c,4a,4b] most of the nucleophiles investigated favor Markovnikov-selective nucleopalladation. Surprisingly, the EDA results indicate that the kinetic regioselectivity of nucleopalladation is not very sensitive to the steric properties of the nucleophile. For example, nucleopalladations with sterically distinct primary amines (NH_2Me, NH_2iPr, and NH_2tBu in Figure 8a–c)[4a,36] have comparable contributions resulting from steric effects ($\Delta\Delta E_{steric}$ = 6.1~6.9 kcal/mol). These nucleopalladations are all kinetically Markovnikov-selective, because the sum of electronic and dispersion effects in these reactions is greater than the steric influences. These results are consistent with previous experimental reports that suggest reactions with relatively bulky *N*-nucleophiles, such as NHMe[2,4a] still prefer Markovnikov products. Only in the reaction with an extremely bulky secondary amine nucleophile ($NHiPr_2$ in Figure 8d), the $\Delta\Delta E_{steric}$ is

significantly increased and reverses the regioselectivity to favor the *anti*-Markovnikov addition products. Similarly, nucleopalladations with MeOH and *t*BuOH also have comparable $\Delta\Delta E_{steric}$ terms (7.7 and 8.3 kcal/mol in Figure 8e–f, respectively).[37]

The insensitivity of nucleophile steric effects underlines the challenge to achieve *anti*-Markovnikov selectivity with the neutral $Pd(OAc)_2$ catalyst. It also highlighted the importance of understanding the origin of electronic effects because electrostatic interactions and orbital interactions may be more tunable. Interestingly, the magnitudes of the electrostatic effects are sensitive to the formal charge of the nucleophile. Nucleopalladations with negatively charged nucleophiles (Figure 8g–h and 7b), such as CH_3CO_{2-}, CF_3CO_{2-}, and PhthN−, have much more negative $\Delta\Delta E_{elstat}$ than those with neutral nucleophiles. These results indicate that anionic nucleophiles tend to lead to greater Markovnikov selectivity due to more favorable nucleophile-alkene electrostatic attraction in the Markovnikov addition transition state (Figure 1a). On the other hand, the nucleophilicity of the nucleophile have a small impact on the regioselectivity. For example, the $\Delta\Delta E_{elstat}$ and $\Delta\Delta E_{orbital}$ values are almost identical for nucleopalladations with CH_3CO_{2-} and CF_3CO_{2-} (Figure 8g–h), although the former is expected to beslightly more nucleophilic. The similar $\Delta\Delta E_{elstat}$ and $\Delta\Delta E_{orbital}$ values of nucleopalladations with PhthN− and acetate anion indicate the *N*- and *O*-nucleophiles have similar electronic effects.[38] On the other hand, *O*-nucleophiles, including alcohols and carboxylate anions, have slightly greater $\Delta\Delta E_{steric}$ terms (by ~1 kcal/mol) than primary amine nucleophiles. This is likely due to the shorter C−O bonds in the *O*-addition transition states that make these processes more sensitive to nucleophile-substrate steric repulsions.

Taken together, these EDA results indicate that in the neutral $Pd(OAc)_2$-mediated nucleopalladations, the different types of nucleophile-substrate interactions have different sensitivity to the steric and electronic properties of the nucleophile. Nucleophilesubstrate steric interactions are largely insensitive to the size of the nucleophile, unless a highly hindered secondary amine is used. Although nucleophile-substrate orbital interactions remain nearly constant in all *trans*-aminopalladation processes tested, the nucleophile-substrate electrostatic interactions are highly sensitive to the formal charge of the nucleophiles. In reactions with negatively charged nucleophiles, such as CH_3CO_{2-}, CF_3CO_{2-}, and PhthN−, electrostatic effects provide the greatest contribution to the Markovnikov selectivity, while in reactions with neutral nucleophiles, including various primary amines and alcohols, contributions from electrostatics and orbital interactions are comparable. The only case where steric effects dominate and thus favor the *anti*-Markovnikov pathway is with the highly hindered $NHiPr_2$ nucleophile.

Catalyst effects on the regioselectivity

The EDA results discussed above indicated the $Pd(OAc)_2$- mediated nucleopalladation with a large majority of nucleophiles favors the Markovnikov pathway. Therefore, the regiochemical reversal with the anionic Pd catalyst to *kinetically* favor the *anti*-Markovnikov nucleopalladation is remarkably unique. To investigate the origin of the catalyst-controlled regioselectivity, we performed EDA analysis on the regioselectivity of nucleopalladation with various neutral and anionic Pd catalysts. The use of another neutral Pd catalyst,

$Pd(H_2O)Cl_2$, a potential active catalyst in Wacker oxidations,[1c] leads to similar regioselectivities compared to those with $Pd(OAc)_2$ discussed above. Reactions with $Pd(H_2O)Cl_2$ are also relatively insensitive to the steric property and nucleophilicity, while more sensitive to the formal charge of the nucleophile (See Figure S20 for details). In contrast, EDA analysis with the anionic palladate $Pd(OAc)_{3-}$ as the active catalyst indicated a substantially different regioselectivity control (Figure 9). In particular, the comparison between $Pd(OAc)_{3-}$- and $Pd(OAc)_2$-mediated *trans*-aminopalladation with phthalimide anion as nucleophile (Figures 9 and 7b, respectively) reveals the origin of the different regioselectivity with anionic and neutral Pd catalysts. The complete reversal of regioselectivity to favor the *anti*-Markovnikov products is mainly attributed to the decrease of electrostatic effects in the reaction with the anionic Pd catalyst ($\Delta\Delta E_{elstat}$ = −2.5 kcal/mol foranionic Pd versus −5.4 kcal/mol for the neutral Pd system).

These results indicate the electronic properties of the Pd catalyst can alter the polarization of the electron-density of the alkene in the π-alkene complex. This hypothesis is supported by the CHelpG atomic charge[34,39] calculations (Figure 9). With the more electronrich anionic palladate, the ligand-to-metal charge transfer[40] is less significant, and thus the internal carbon of the alkene in complex **11** becomes more electron-rich than that in **5** (Figure 7b). Therefore, the attractive electrostatic interactions between the nucleophile and the internal carbon becomes less favorable with the anionic palladium catalyst due to the decreased polarization of the C=C double bond in the π-alkene complex **11**. Because the electrostatic and orbital interaction effects are both small in this anionic Pd catalyst system, steric effects become the dominant factor and effectively override the effects of orbital interactions, electrostatics, and dispersion to favor the *anti*-Markovnikov addition. EDA studies with other anionic palladate complexes, *e.g.* $PdCl(OAc)_{2-}$, $Pd(OPiv)_{3-}$, $Pd(TFA)_{3-}$, also support the same conclusion that aminopalladations with anionic palladate complexes have diminished electronic effects on regioselectivity, and thus steric effects are the dominant factor leading to the *anti*-Markovnikov selective products (See Figure S14 and S18 for details).

Summary of the catalyst effects and nucleophile effects on the regioselectivity

The dominant factors controlling the kinetic regioselectivity in nucleopalladation with different Pd catalysts and nucleophiles are summarized in Figure 10. Although a majority of *N*- and *O*nucleophiles favor the Markovnikov-selective nucleopalladation when reacting with a neutral π-alkene/Pd(II) complex, the dominant factor on regioselectivity can be distinct. For nucleophiles that undergo *cis*-nucleopalladation (**TS-e**), the favorable π→d orbital interactions are the most important factor that leads to the Markovnikov selectivity. In *trans*-nucleopalladation with anionic nucleophiles (**TS-c**), electrostatic effects ($\Delta\Delta E_{elstat}$) become the most important factor favoring the Markovnikov selectivity. In *trans*nucleopalladation with neutral nucleophiles (**TS-d**), both orbital interactions and electrostatics are the main effects controlling the regioselectivity. In contrast, *anti*-Markovnikov-selective nucleopalladation is favored when steric effects ($\Delta\Delta E_{steric}$) dominate. Our computational analysis suggests the regioselectivity is relatively insensitive to the steric properties of the nucleophile. Therefore, only highly bulky nucleophiles (**TS-b**) can override the intrinsic electronic preference and selectively form the *anti*-Markovnikov products. On

the other hand, because the nucleophile-substrate electrostatic interactions are sensitive to the formal charges on the Pd catalyst, the use of anionic palladate catalysts (**TS-a**) significantly reduces the effects of electrostatic interactions that favor the Markovnikov addition. Therefore, the nucleophile-substrate steric repulsions become the dominant factor in these reaction systems, leading to the catalyst-controlled complete reversal of regioselectivity.

CONCLUSION

We presented an energy decomposition approach to separate different types of nucleophile-substrate interactions and to rationalize their contributions to the regioselectivity of the nucleopalladation of terminal aliphatic alkenes. The computed regioselectivity ($\Delta\Delta E^{\ddagger}$) is quantitatively dissected into effects from steric repulsions ($\Delta\Delta E_{steric}$), electrostatics ($\Delta\Delta E_{elstat}$), orbital interactions ($\Delta\Delta E_{orbital}$), and dispersion ($\Delta\Delta E_{disp}$) between the nucleophile and the alkene in the nucleopalladation transition state. Therefore, the major factor controlling the regioselectivity of reactions with different catalysts and nucleophiles can be revealed in a robust and practical fashion.

In this study, we employed this approach to study the origins of regioselectivity in a series of nucleopalladation reactions with neutral and anionic Pd catalysts and different nucleophiles. The computational results indicated that the regioselectivity is largely insensitive to the steric property of the nucleophile, unless an extremely bulky nucleophile is used. On the other hand, the nucleophilesubstrate electrostatic interactions and orbital interactions can be affected by the electronic properties of the nucleophile and the Pd catalyst, and the *cis*/*trans*-nucleopalladation mechanisms. In $Pd(OAc)_2$-mediated *cis*-nucleopalladation, the Markovnikov selectivity is mainly due to the favorable frontier molecular orbital interactions between the Pd-nucleophile complex and the alkene substrate. In $Pd(OAc)_2$-mediated *trans*-nucleopalladation, the orbital interaction effects are diminished and the favorable electrostatic interactions with the internal carbon of the alkene becomes more important for the Markovnikov-selectivity. The use of an anionic palladate catalyst decreases the polarization of the π electrondensity of the alkene, and thus the electrostatic effects are diminished. Therefore, the catalyst-controlled *anti*-Markovnikov selectivity in Hull's oxidative amination reactions is due to the diminished electrostatic effect that makes steric effects the dominant factor on regioselectivity. We expect the interplay of steric, electrostatic, and orbital interaction effects on regioselectivity of alkene nucleometallation revealed in this study can offer unique insights to guide future experimental design of regiodivergent functionalization strategies of simple unactivated alkenes. For example, since the electrostatic effect on regioselectivity appears to be more easily tunable, strategies to suppress the favorable electrostatic interactions in Markovnikov attack may lead to greater levels of anti-Markovnikov selectivity. This may be achieved through further optimization of electronic properties of the active Pd catalyst. Furthermore, the energy decomposition approach described here may be applied to study the origin of reactivity, regio-, and stereoselectivity of other types of transition metal-catalyzed reactions.

Supplementary Material

Refer to Web version on PubMed Central for supplementary material.

ACKNOWLEDGMENT

We thank the NIH (R35GM128779 and R35GM125029) for financial support for this work. Calculations were performed at the Center for Research Computing at the University of Pittsburgh and the Extreme Science and Engineering Discovery Environment (XSEDE) supported by the NSF. We also thank Prof. Daniel S. Lambrecht at the University of Pittsburgh for helpful discussions.

REFERENCES

(1). (a)Bäckvall J-E Palladium in some selective oxidation reactions. Acc. Chem. Res 1983, 16, 335–342;(b)Schafer LL; Yim JCH; Yonson N Transition-Metal-Catalyzed Hydroamination Reactions. 2013, Transition-Metal-Catalyzed Hydroamination Reactions. Metal-Catalyzed Cross-Coupling Reactions and More; Wiley-VCH: Weinheim; pp 1135–1258;(c)Kočovsky P; Bäckvall J-E The syn/anti-dichotomy in the palladiumcatalyzed addition of nucleophiles to alkenes. Chem.-Eur. J 2015, 21, 36–56; [PubMed: 25378278] (d)Yin G; Mu X; Liu G Palladium(II)-Catalyzed Oxidative Difunctionalization of Alkenes: Bond Forming at a High-Valent Palladium Center. Acc. Chem. Res 2016, 49, 2413–2423. [PubMed: 27739689]

(2). (a)McDonald RI; Liu G; Stahl SS Palladium(II)-catalyzed alkene functionalization via nucleopalladation: stereochemical pathways and enantioselective catalytic applications. Chem. Rev 2011, 111, 2981–3019; [PubMed: 21428440] (b)Garlets ZJ; White DR; Wolfe JP Recent Developments in Pd0-Catalyzed Alkene-Carboheterofunctionalization Reactions. Asian J. Org. Chem 2017, 6, 636–653. [PubMed: 29130026]

(3). For regioselective nucleopalladation using Lewis-basic directing groups or in intramolecular reactions, see:(a)Weiner B; Baeza A; Jerphagnon T; Feringa BL Aldehyde selective Wacker oxidations of phthalimide protected allylic amines: a new catalytic route to beta3-amino acids. J. Am. Chem. Soc 2009, 131, 9473–9474; [PubMed: 19583430] (b)Gurak JA Jr.; Yang KS; Liu Z; Engle KM Directed, Regiocontrolled Hydroamination of Unactivated Alkenes via Protodepalladation. J. Am. Chem. Soc 2016, 138, 5805–5808; [PubMed: 27093112] (c)Gurak JA; Engle KM Regioselective Hydroamination Using a Directed Nucleopalladation/ Protodepalladation Strategy. Synlett 2017, 28, 2057–2065;(d)ref. 2b.

(4). (a)Åkermark B; Bäckvall JE; Hegedus LS; Zetterberg K; Siirala-Hansén K; Sjöberg K Palladium-promoted addition of amines to isolated double bonds. J. Organomet. Chem 1974, 72, 127–138; (b)Winstein S; McCaskie J; Lee H-B; Henry PM Oxidation of olefins by palladium(II). 9. Mechanism of the oxidation of olefins by the dimeric species, disodium dipalladium hexaacetate, in acetic acid. J. Am. Chem. Soc 1976, 98, 6913–6918;(c)Andell OS; Bäckvall J-E Evidence for transacetoxypalladation of alkenes in chloride-free media. J. Organomet. Chem 1983, 244, 401–407;(d)Brice JL; Harang JE; Timokhin VI; Anastasi NR; Stahl SS Aerobic oxidative amination of unactivated alkenes catalyzed by palladium. J. Am. Chem. Soc 2005, 127, 2868–2869; [PubMed: 15740119] (e)Baiju TV; Gravel E; Doris E; Namboothiri INN Recent developments in Tsuji-Wacker oxidation. Tetrahedron Lett 2016, 57, 3993–4000.

(5). (a)Eisenstein O; Hoffmann R Activation of a coordinated olefin toward nucleophilic attack. J. Am. Chem. Soc 1980, 102, 6148–6149;(b)Eisenstein O; Hoffmann R Transition-metal complexed olefins: how their reactivity toward a nucleophile relates to their electronic structure. J. Am. Chem. Soc 1981, 103, 4308–4320;(c)Bäckvall J-E; Bjoerkman EE; Pettersson L; Siegbahn P Reactivity of coordinated nucleophiles toward cis migration in (.pi.-olefin)palladium complexes. J. Am. Chem. Soc 1984, 106, 4369–4373;(d)Bäckvall J-E; Bjoerkman EE; Pettersson L; Siegbahn P A theoretical study on the reactivity of nucleophiles coordinated to palladium. J. Am. Chem. Soc 1985, 107, 7265–7267.

(6). Timokhin VI; Stahl SS Bronsted base-modulated regioselectivity in the aerobic oxidative amination of styrene catalyzed by palladium. J. Am. Chem. Soc 2005, 127, 17888–17893. [PubMed: 16351120]

(7). (a)Xu X; Liu P; Lesser A; Sirois LE; Wender PA; Houk KN Ligand effects on rates and regioselectivities of Rh(I)-catalyzed (5 + 2) cycloadditions: a computational study of cyclooctadiene and dinaphthocyclooctatetraene as ligands. J. Am. Chem. Soc 2012, 134, 11012–11025; [PubMed: 22668243] (b)Kumar M; Chaudhari RV; Subramaniam B; Jackson TA Ligand Effects on the Regioselectivity of Rhodium-Catalyzed Hydroformylation: Density Functional Calculations Illuminate the Role of Long-Range Noncovalent Interactions. Organometallics 2014, 33, 4183–4191;(c)Lyngvi E; Sanhueza IA; Schoenebeck F Dispersion Makes the Difference: Bisligated Transition States Found for the Oxidative Addition of Pd(PtBu3)2 to Ar-OSO2R and Dispersion-Controlled Chemoselectivity in Reactions with Pd[P(iPr)(tBu2)]2. Organometallics 2014, 34, 805–812.

(8). (a)Xing D; Qi X; Marchant D; Liu P; Dong G Branched-Selective Direct alpha-Alkylation of Cyclic Ketones with Simple Alkenes. Angew. Chem. Int. Ed 2019, 58, doi: 10.1002/anie.201900301;(b)Carbo JJ; Maseras F; Bo C; van Leeuwen PWNM Unraveling the origin of regioselectivity in rhodium diphosphine catalyzed hydroformylation. A DFT QM/MM study. J. Am. Chem. Soc 2001, 123, 7630–7637; [PubMed: 11480985] (c)Huang G; Liu P Mechanism and Origins of Ligand-Controlled Linear Versus Branched Selectivity of Iridium-Catalyzed Hydroarylation of Alkenes. ACS Catal 2016, 6, 809–820;(d)Li X; Wu H; Lang Y; Huang G Mechanism, selectivity, and reactivity of iridium- and rhodium-catalyzed intermolecular ketone α-alkylation with unactivated olefins via an enamide directing strategy. Catal. Sci. Technol 2018, 8, 2417–2426.

(9). Couce-Rios A; Lledos A; Ujaque G The Origin of Anti-Markovnikov Regioselectivity in Alkene Hydroamination Reactions Catalyzed by [Rh(DPEphos)]+. Chem.-Eur. J 2016, 22, 9311–9320. [PubMed: 27226329]

(10). (a)Liu G; Stahl SS Highly regioselective Pd-catalyzed intermolecular aminoacetoxylation of alkenes and evidence for cisaminopalladation and S(N)2 C-O bond formation. J. Am. Chem. Soc 2006, 128, 7179–7181; [PubMed: 16734468] (b)Keith JA; Henry PM The mechanism of the Wacker reaction: a tale of two hydroxypalladations. Angew. Chem. Int. Ed 2009, 48, 9038–9049.

(11). (a)Ess DH; Houk KN Distortion/interaction energy control of 1,3-dipolar cycloaddition reactivity. J. Am. Chem. Soc 2007, 129, 10646–10647; [PubMed: 17685614] (b)Fernandez I; Bickelhaupt FM The activation strain model and molecular orbital theory: understanding and designing chemical reactions. Chem. Soc. Rev 2014, 43, 4953–4967; [PubMed: 24699791] (c)Liu S; Lei Y; Qi X; Lan Y Reactivity for the Diels-Alder reaction of cumulenes: a distortioninteraction analysis along the reaction pathway. J. Phys. Chem. A 2014, 118, 2638–2645; [PubMed: 24576078] (d)Bickelhaupt FM; Houk KN Analyzing Reaction Rates with the Distortion/Interaction-Activation Strain Model. Angew. Chem. Int. Ed 2017, 56, 10070–10086.

(12). (a)Kitaura K; Morokuma K A new energy decomposition scheme for molecular interactions within the Hartree-Fock approximation. Int. J. Quantum Chem 1976, 10, 325–340;(b)Ziegler T; Rauk A A theoretical study of the ethylene-metal bond in complexes between copper(1+), silver(1+), gold(1+), platinum(0) or platinum(2+) and ethylene, based on the Hartree-Fock-Slater transition-state method. Inorg. Chem 1979, 18, 1558–1565;(c)Dorigo AE; Morokuma K Theoretical studies of nucleophilic additions of organocopper reagents to acrolein. Rationalization of the differences in regioselectivity in the reactions of methylcopper and methyllithium. J. Am. Chem. Soc 1989, 111, 4635–4643;(d)Nakamura E; Miyachi Y; Koga N; Morokuma K Theoretical studies of heteroatom-directed carbometalation. Addition of methylcopper, dimethylcopper anion, and methyllithium to substituted acetylenes. J. Am. Chem. Soc 1992, 114, 6686–6692;(e)Ess DH; Goddard WA; Periana RA Electrophilic, Ambiphilic, and Nucleophilic C−H Bond Activation: Understanding the Electronic Continuum of C−H Bond Activation Through Transition-State and Reaction Pathway Interaction Energy Decompositions. Organometallics 2010, 29, 6459–6472;(f)Hopffgarten M. v.; Frenking G Energy decomposition analysis. Wiley Interdisciplinary Reviews: Computational Molecular Science 2012, 2, 43–62.

(13). Kohler DG; Gockel SN; Kennemur JL; Waller PJ; Hull KL Palladium-catalysed anti-Markovnikov selective oxidative amination. Nat. Chem 2018, 10, 333–340. [PubMed: 29461537]

(14). (a)Keith JA; Nielsen RJ; Oxgaard J; Goddard WA J. Am. Chem. Soc 2007, 129, 12342; [PubMed: 17880213] (b)Dewan A; Bharali P; Bora U; Thakur AJ Starch assisted Palladium(0) nanoparticles as in situ generated catalysts for room temperature Suzuki-Miyaura reaction in water. RSC Adv 2016, 6, 11758;(c)Shishilov ON; Stromnova TA; Churakov AV; Kuz'mina LG;

Efimenko IA Palladium Acetate Complexes with Morpholine and 4-Methylmorpholine. The Structure of $Pd(C_4H_9ON)_2(OAc)_2{\cdot}2H_2O$. Russ. J. Inorg. Chem 2006, 51, 626–632;(d)Amatore C; Jutand A Anionic Pd(0) and Pd(II) Intermediates in Palladium-Catalyzed Heck and Cross-Coupling Reactions. Acc. Chem. Res 2000, 33, 314–321; [PubMed: 10813876] (e)Xue L; Lin Z Theoretical aspects of palladiumcatalysed carbon-carbon cross-coupling reactions. Chem. Soc. Rev 2010, 39, 1692–1705. [PubMed: 20419215]

(15). (a)Schroeter F; Strassner T Understanding Anionic “Ligandless” Palladium Species in the Mizoroki-Heck Reaction. Inorg. Chem 2018, 57, 5159–5173; [PubMed: 29671325] (b)Schroeter F; Soellner J; Strassner T Cross-Coupling Catalysis by an Anionic Palladium Complex. ACS Catal 2017, 7, 3004–3009;(c)Droll HA; Block BP; Fernelius WC Studies on Coördination Compounds. XV. Formation Constants for Chloride and Acetylacetonate Complexes of Palladium(II). J. Phys. Chem 1957, 61, 1000–1004.

(16). (a)Diefenbach A; de Jong GT; Bickelhaupt FM Activation of H-H, C-H, C-C and C-Cl Bonds by Pd and PdCl(−). Understanding Anion Assistance in C-X Bond Activation. J. Chem. Theory Comput 2005, 1, 286–298; [PubMed: 26641300] (b)Carrow BP; Hartwig JF Ligandless, anionic, arylpalladium halide intermediates in the Heck reaction. J. Am. Chem. Soc 2010, 132, 79–81. [PubMed: 20014842]

(17). Frisch MJ; Trucks GW; Schlegel HB; Scuseria GE; Robb MA; Cheeseman JR; Scalmani G; Barone V; Mennucci B; Petersson GA; Nakatsuji H; Caricato M; Li X; Hratchian HP; Izmaylov AF; Bloino J; Zheng G; Sonnenberg JL; Hada M; Ehara M; Toyota K; Fukuda R; Hasegawa J; Ishida M; Nakajima T; Honda Y; Kitao O; Nakai H; Vreven T; Montgomery JA Jr.; Peralta JE; Ogliaro F; Bearpark M; Heyd JJ; Brothers E; Kudin KN; Staroverov VN; Kobayashi R; Normand J; Raghavachari K; Rendell A; Burant JC; Iyengar SS; Tomasi J; Cossi M; Rega N; Millam NJ; Klene M; Knox JE; Cross JB; Bakken V; Adamo C; Jaramillo J; Gomperts R; Stratmann RE; Yazyev O; Austin AJ; Cammi R; Pomelli C; Ochterski JW; Martin RL; Morokuma K; Zakrzewski VG; Voth GA; Salvador P; Dannenberg JJ; Dapprich S; Daniels AD; Farkas O; Foresman JB; Ortiz JV; Cioslowski J; Fox DJ, Gaussian 09, Revision D.01; Gaussian, Inc.: Wallingford, CT, 2013.

(18). (a)Lee C; Yang W; Parr RG Development of the Colle-Salvetti correlation-energy formula into a functional of the electron density. Phys. Rev. B 1988, 37, 785–789;(b)Becke AD Density-functional thermochemistry. III. The role of exact exchange. J. Chem. Phys 1993, 98, 5648–5652.

(19). Ribeiro RF; Marenich AV; Cramer CJ; Truhlar DG Use of solution-phase vibrational frequencies in continuum models for the free energy of solvation. J. Phys. Chem. B 2011, 115, 14556–14562. [PubMed: 21875126]

(20). Marenich AV; Cramer CJ; Truhlar DG Universal solvation model based on solute electron density and on a continuum model of the solvent defined by the bulk dielectric constant and atomic surface tensions. J. Phys. Chem. B 2009, 113, 6378–6396. [PubMed: 19366259]

(21). Zhao Y; Truhlar DG The M06 suite of density functionals for main group thermochemistry, thermochemical kinetics, noncovalent interactions, excited states, and transition elements: two new functionals and systematic testing of four M06-class functionals and 12 other functionals. Theor. Chem. Acc 2007, 120, 215–241.

(22). (a)Khaliullin RZ; Cobar EA; Lochan RC; Bell AT; Head-Gordon M Unravelling the origin of intermolecular interactions using absolutely localized molecular orbitals. J. Phys. Chem. A 2007, 111, 8753–8765; [PubMed: 17655284] (b)Horn PR; Mao Y; Head-Gordon M Defining the contributions of permanent electrostatics, Pauli repulsion, and dispersion in density functional theory calculations of intermolecular interaction energies. J. Chem. Phys 2016, 144, 114107; [PubMed: 27004862] (c)Horn PR; Mao Y; Head-Gordon M Probing non-covalent interactions with a second generation energy decomposition analysis using absolutely localized molecular orbitals. Phys. Chem. Chem. Phys 2016, 18, 23067–23079; [PubMed: 27492057] (d)Mao Y; Demerdash O; Head-Gordon M; Head-Gordon T Assessing Ion-Water Interactions in the AMOEBA Force Field Using Energy Decomposition Analysis of Electronic Structure Calculations. J. Chem. Theory Comput 2016, 12, 5422–5437. [PubMed: 27709939]

(23). Shao Y; Gan Z; Epifanovsky E; Gilbert ATB; Wormit M; Kussmann J; Lange AW; Behn A; Deng J; Feng XT; Ghosh D; Goldey M; Horn PR; Jacobson LD; Kaliman I; Khaliullin RZ; Kus T; Landau A; Liu J; Proynov EI; Rhee YM; Richard RM; Rohrdanz MA; Steele RP; Sundstrom EJ; Woodcock HL; Zimmerman PM; Zuev D; Albrecht B; Alguire E; Austin B; Beran GJO; Bernard

YA; Berquist E; Brandhorst K; Bravaya KB; Brown ST; Casanova D; Chang CM; Chen YQ; Chien SH; Closser KD; Crittenden DL; Diedenhofen M; DiStasio RA; Do H; Dutoi AD; Edgar RG; Fatehi S; Fusti-Molnar L; Ghysels A; Golubeva-Zadorozhnaya A; Gomes J; Hanson-Heine MWD; Harbach PHP; Hauser AW; Hohenstein EG; Holden ZC; Jagau TC; Ji HJ; Kaduk B; Khistyaev K; Kim J; Kim J; King RA; Klunzinger P; Kosenkov D; Kowalczyk T; Krauter CM; Lao KU; Laurent AD; Lawler KV; Levchenko SV; Lin CY; Liu F; Livshits E; Lochan RC; Luenser A; Manohar P; Manzer SF; Mao SP; Mardirossian N; Marenich AV; Maurer SA; Mayhall NJ; Neuscamman E; Oana CM; Olivares-Amaya R; O'Neill DP; Parkhill JA; Perrine TM; Peverati R; Prociuk A; Rehn DR; Rosta E; Russ NJ; Sharada SM; Sharma S; Small DW; Sodt A; Stein T; Stuck D; Su YC; Thom AJW; Tsuchimochi T; Vanovschi V; Vogt L; Vydrov O; Wang T; Watson MA; Wenzel J; White A; Williams CF; Yang J; Yeganeh S; Yost SR; You ZQ; Zhang IY; Zhang X; Zhao Y; Brooks BR; Chan GKL; Chipman DM; Cramer CJ; Goddard WA; Gordon MS; Hehre WJ; Klamt A; Schaefer HF; Schmidt MW; Sherrill CD; Truhlar DG; Warshel A; Xu X; Aspuru-Guzik A; Baer R; Bell AT; Besley NA; Chai JD; Dreuw A; Dunietz BD; Furlani TR; Gwaltney SR; Hsu CP; Jung YS; Kong J; Lambrecht DS; Liang WZ; Ochsenfeld C; Rassolov VA; Slipchenko LV; Subotnik JE; Van Voorhis T; Herbert JM; Krylov AI; Gill PMW; Head-Gordon M Advances in molecular quantum chemistry contained in the Q-Chem 4 program package. Mol. Phys 2015, 113, 184–215.

(24). (a)Khaliullin RZ; Bell AT; Head-Gordon M Analysis of charge transfer effects in molecular complexes based on absolutely localized molecular orbitals. J. Chem. Phys 2008, 128, 184112; [PubMed: 18532804] (b)Khaliullin RZ; Bell AT; Head-Gordon M Electron donation in the water-water hydrogen bond. Chem.-Eur. J 2009, 15, 851–855. [PubMed: 19086050]

(25). Legault CY CYLView, 1.0b; Université de Sherbrooke, Canada, http://www.cylview.org.

(26). See Figure S2 in SI for the proposed aminopalladation and allylic C–H activation pathways for Pd-catalyzed oxidative amination of alkenes. The allylic C–H activation mechanism was ruled out by experimental deuterium labeling and kinetic isotope effects studies (Figure 2b). Our DFT calculations also indicated the allylic C–H acti-vation pathway requires a much higher barrier than the aminopalladation pathways. .

(27). DFT results suggested that the β-hydride elimination and alkene isomerization all require lower activation free energy barrier. See Figure S7 in SI for the detailed free energy profiles.

(28). The phthalimide anion is formed by the deprotonation of phthalimide using acetate anion. This step requires only 1.6 kcal/mol, indicating a facile equilibrium for the deprotonation process. See Figure S1 for details.

(29). Dimeric palladate complexes may also be formed under these conditions. Our calculations indicate the monomeric and dimeric palladate complexes, such as $Pd(OAc)_{3-}$ and $Pd_2(OAc)_{5-}$, have comparable stabilities and may exist in an equilibrium. In addition, one or more of the acetate ligands maybe replaced by other anions, such as Cl− and PhthN−. Thus, the reaction may proceed with multiple monomeric and dimeric palladate complexes as the active catalysts. To simplify the calculations, we chose $Pd(OAc)_{3-}$ and $Pd_2(OAc)_{5-}$ as model monomeric and dimeric catalysts to investigate the mechaisms for aminopalladation. Due to unfavorable steric repulsions between the bulky $Pd_2(OAc)_{5-}$ catalyst and the internal alkenyl carbon, the $Pd_2(OAc)_{5-}$ π-alkene complex is less reactive in the anti-Markovnikov aminopalladation than the monomeric $Pd(OAc)_3$-π-alkene complex 11. Thus, only the monomeric pathway was discussed in detail in the main text. See Figure S3 and S4 for detailed discussions about the potential roles of the dimeric palladate complexes.

(30). Here, the computationally predicted regioselectivity (187:1) is greater than the experimentally observed regioselectivity under the optimized reaction conditions (25 mol % Bu_4NCl and 15 mol % Bu_4NOAc). This may be due to the competing Markovnikov-selective background reactions catalyzed by the neutral palladium catalyst. Experimentally, a higher concentration of the Bu_4NOAc and Bu_4NCl additives leads to up to 130:1 anti-Markovnikov regioselectivity, albeit with decreased reaction yield.

(31). Here, the orbital interactions term ($\Delta\Delta E_{orbital}$) includes the sum of polarization and charge transfer interactions. In our EDA studies, we found polarization and charge transfer both contribute to the overall regioselectivity and these effects typically favor the same regioisomeric transition state. Therefore, polarization and charge transfer are included as a single term, namely orbital interactions, in subsequent discussions. For other EDA study that combine polarization

and charge transfer into the orbital interactions term, see: Fernandez I; Sola M; Bickelhaupt FM Why do cycloaddition reactions involving C60 prefer [6,6] over [5,6] bonds? Chem.-Eur. J 2013, 19, 7416–7422. . [PubMed: 23576307]

(32). These interfragmental orbital interactions correspond to the charge transfer (ΔE_{ct}) term in eq. 3. The $\Delta\Delta E_{ct}$ term is the major contributor to the orbital interaction energy difference ($\Delta\Delta E_{orbital}$) between **9M-TS** and **9A-TS**. The contribution of intrafragmental polarization ($\Delta\Delta E_{pol}$ = −6.5 kcal/mol) to the regioselectivity is smaller than that of intermolecular charge transfer ($\Delta\Delta E_{ct}$ = −10.6 kcal/mol).

(33). (a)Houk KN Generalized frontier orbitals of alkenes and dienes. Regioselectivity in Diels-Alder reactions. J. Am. Chem. Soc 1973, 95, 4092–4094;(b)Dang L; Zhao H; Lin Z; Marder TB DFT Studies of Alkene Insertions into Cu−B Bonds in Copper(I) Boryl Complexes. Organometallics 2007, 26, 2824–2832.

(34). The CHelpG charges are calculated from fitting the molecular electrostatic potential. Therefore, this charge scheme is expected to provide a better description of the through-space electrostatic interactions with the nucleophile. See: Breneman CM; Wiberg KB Determining atomcentered monopoles from molecular electrostatic potentials. The need forhigh sampling density in formamide conformational analysis. J. Comput. Chem 1990, 1911, 1361–1373.

(35). Hahn C Enhancing electrophilic alkene activation by increasing the positive net charge in transition-metal complexes and application in homogeneous catalysis. Chem.-Eur. J 2004, 10, 5888–5899. [PubMed: 15372675]

(36). The experimental study was performed with $(PhCN)_2PdCl_2$. In the calculations of aminopalladation, $Pd(OAc)_2$ was used as the active catalyst because the same catalyst was used for phthalimide. Both transaminopalladation pathways with and without another amine molecule coordinating to the Pd have been considered in this study. Aminopalladation transition states without another amine coordination are reported here to allow for a direct comparison of the nucleophile effects on regioselectivity. See Figures S8, S9, and S18c for details of the amine-bound pathway.

(37). Here, the predicted kinetic regioselectivity of nucleopalladation with tBuOH favors the Markovnikov product. This is inconsistent with the previously reported $PdCl_2/CuCl_2$-catalyzed anti-Markonikov Wacker oxidation in tBuOH, which favors the aldehyde, albeit with a low yield (<10%). We surmised this reaction likely involves a different active catalyst or a different regioselectivity-determining step, see: Ogura T; Kamimura R; Shiga A; Hosokawa T Reversal of regioselectivity in Wacker-type oxidation of simple terminal alkenes and its paired interacting orbitals (PIO) analysis. Bull. Chem. Soc. Jpn 2005, 78, 1555–1557.

(38). Based on Mayr's nucleophilicity scale, acetate anion and PhthN− have similar nucleophilicities, see:(a)Schaller HF; Tishkov AA; Feng X; Mayr H Direct observation of the ionization step in solvolysis reactions: electrophilicity versus electrofugality of carbocations. J. Am. Chem. Soc 2008, 130, 3012–3022; [PubMed: 18281983] (b)Breugst M; Tokuyasu T; Mayr H Nucleophilic reactivities of imide and amide anions. J. Org. Chem 2010, 75, 5250–5258. [PubMed: 20670031]

(39). Breneman CM; Wiberg KB Determining atom-centered monopoles from molecular electrostatic potentials. The need for high sampling density in formamide conformational analysis. J. Comput. Chem 1990, 11, 361–373.

(40). (a)Dewar JS A Review of the Pi-Complex Theory. Bull. Soc. Chim. Fr 1951, 18, C71–C79; (b)Chatt J; Duncanson LA J. Chem. Soc 1953, 2939–2947;(c)Frenking G; Fröhlich N The Nature of the Bonding in Transition-Metal Compounds. Chem. Rev 2000, 100, 717–774. [PubMed: 11749249]

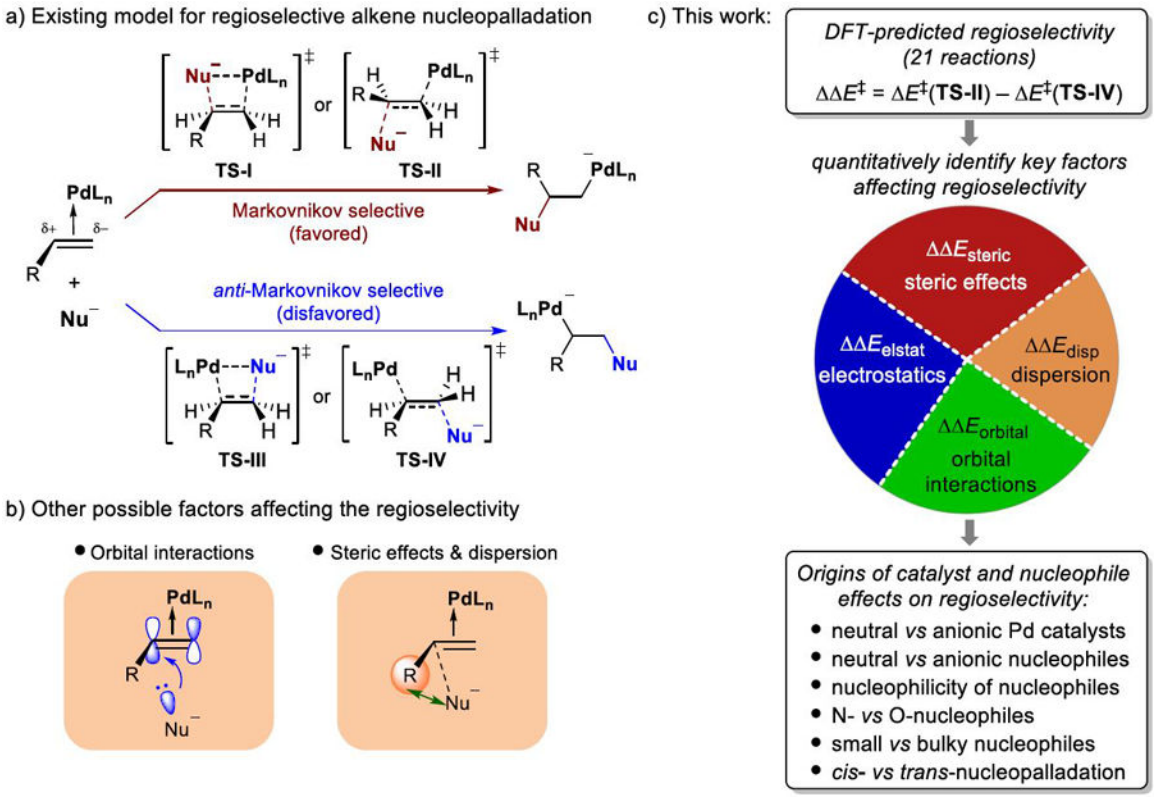

Figure 1.
Factors affecting the regioselectivity of Pd-catalyzed nucleopalladation of alkenes.

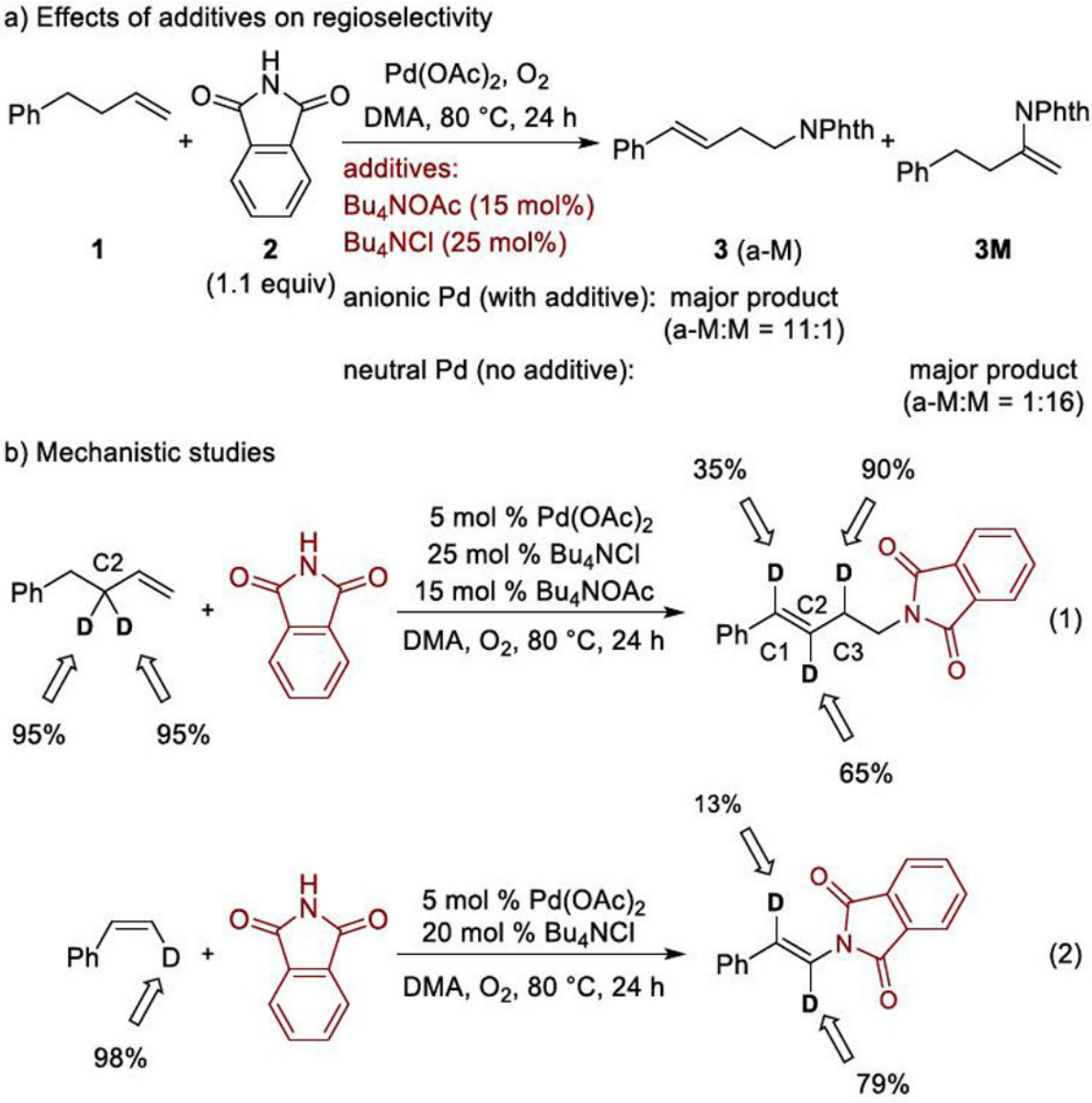

Figure 2.
Pd-catalyzed anti-Markovnikov oxidative amination of alkene

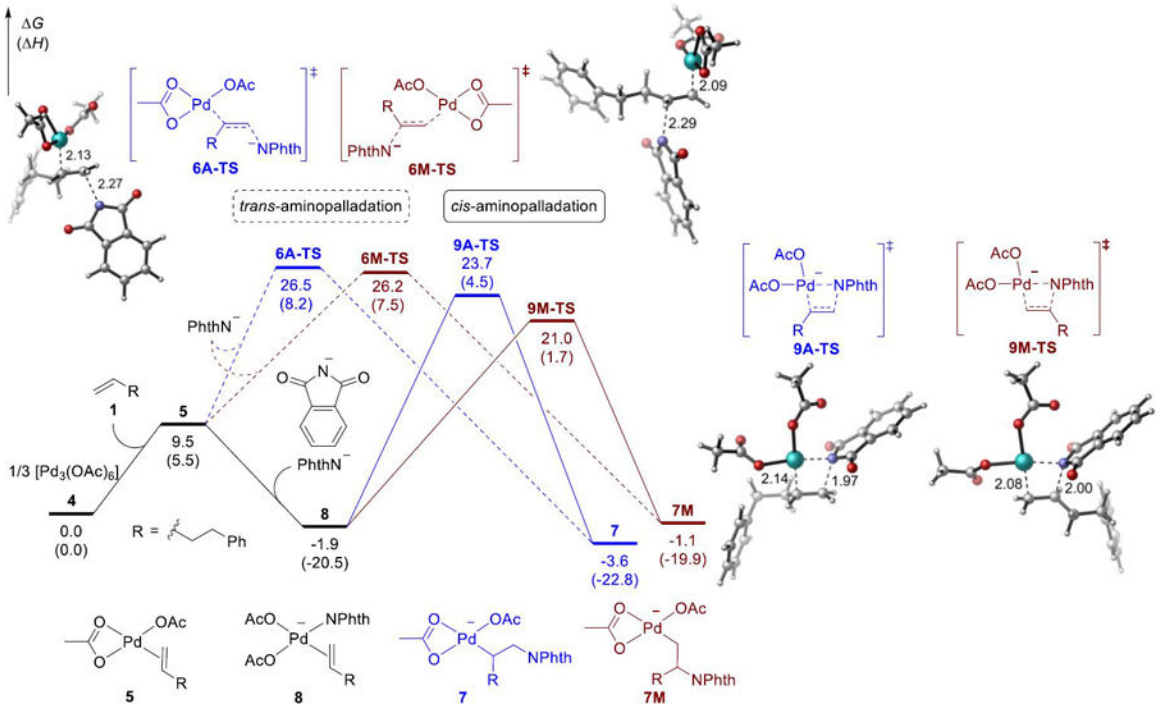

Figure 3.

Free energy profiles of the trans- and cis-aminopalladation pathways with the neutral palladium catalyst. The anti-Markovnikov- and Markovnikov-selective pathways are shown in blue and red, respectively. The energies are in kcal/mol.

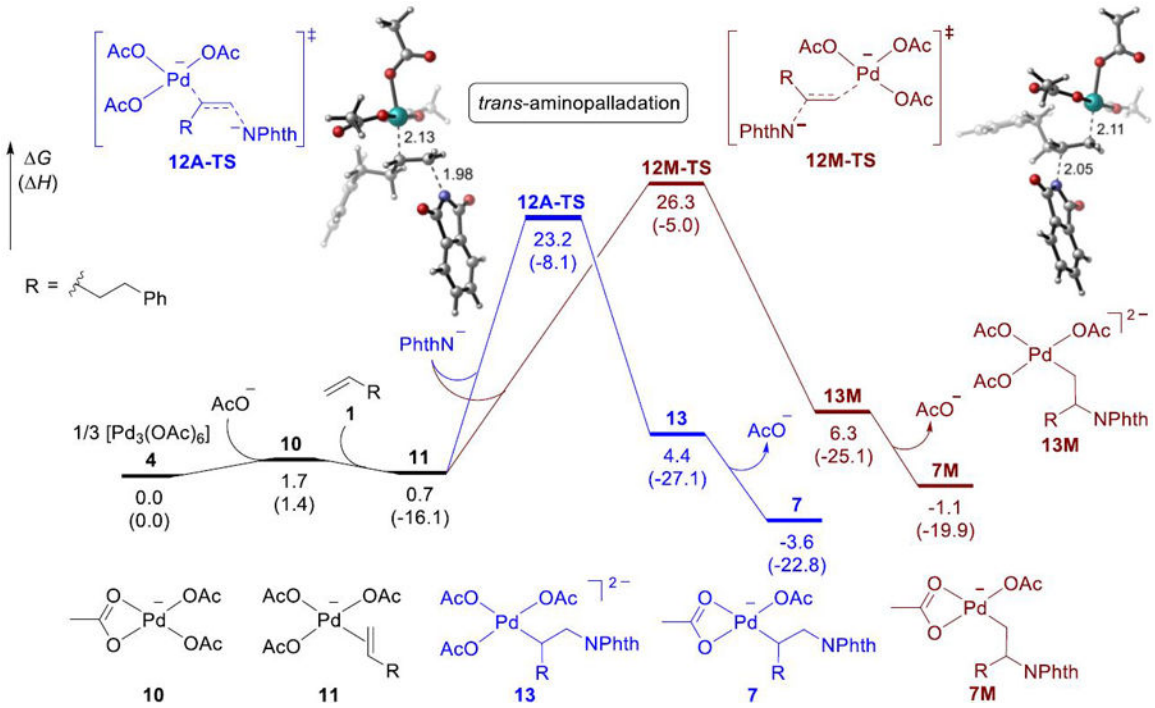

Figure 4.

Free energy profiles of the trans-aminopalladation pathways with the anionic palladate catalyst. The anti-Markovnikov- and Markovnikov- selective pathways are shown in blue and red, respectively. The energies are in kcal/mol.

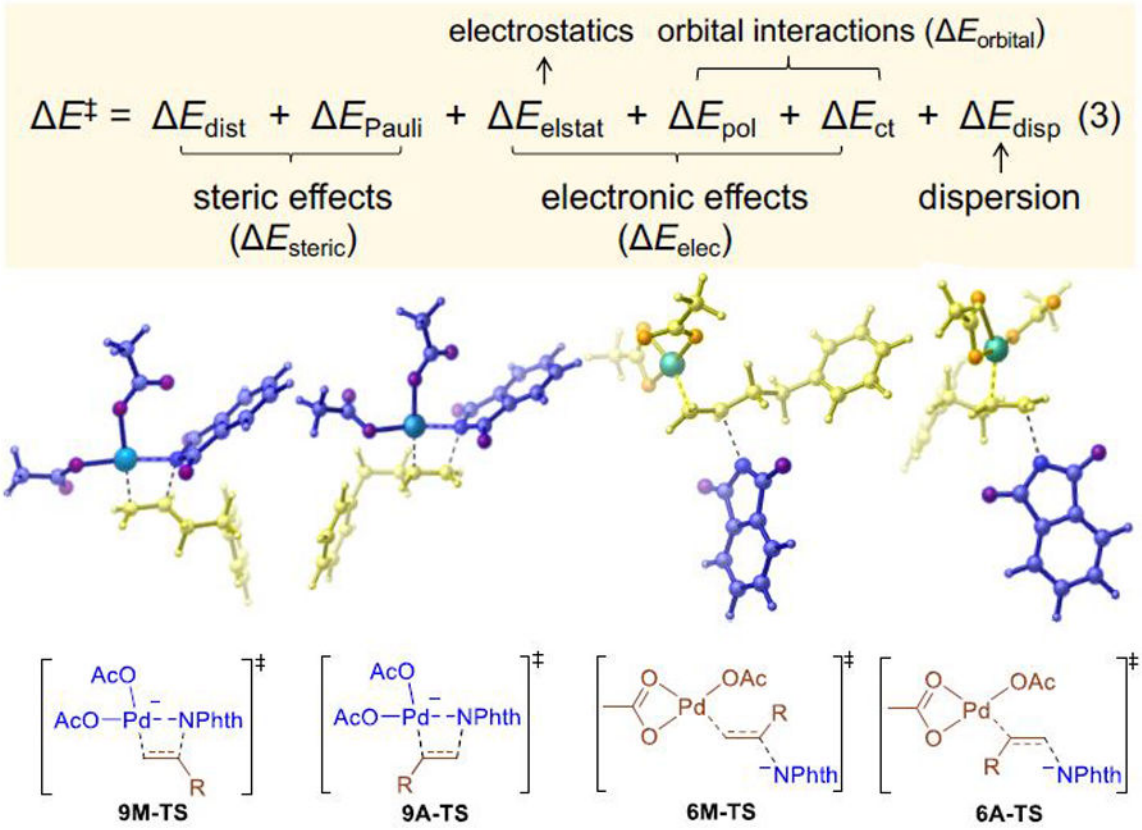

Figure 5.

Decomposition of the activation energies. The steric, electronic, and dispersion interactions between the two highlighted fragments in the aminopalladation transition states are computed using the distortion-interaction model and energy decomposition analysis methods. The two fragments in the EDA calculations of **9M-TS** and **9A-TS** (cis-aminopalladation) are defined as the Pd?Nu complex and the alkene. The two fragments of **6M-TS** and **6A-TS** (transaminopalladation) are defined as the nucleophile and the π-alkene-Pdcomplex.

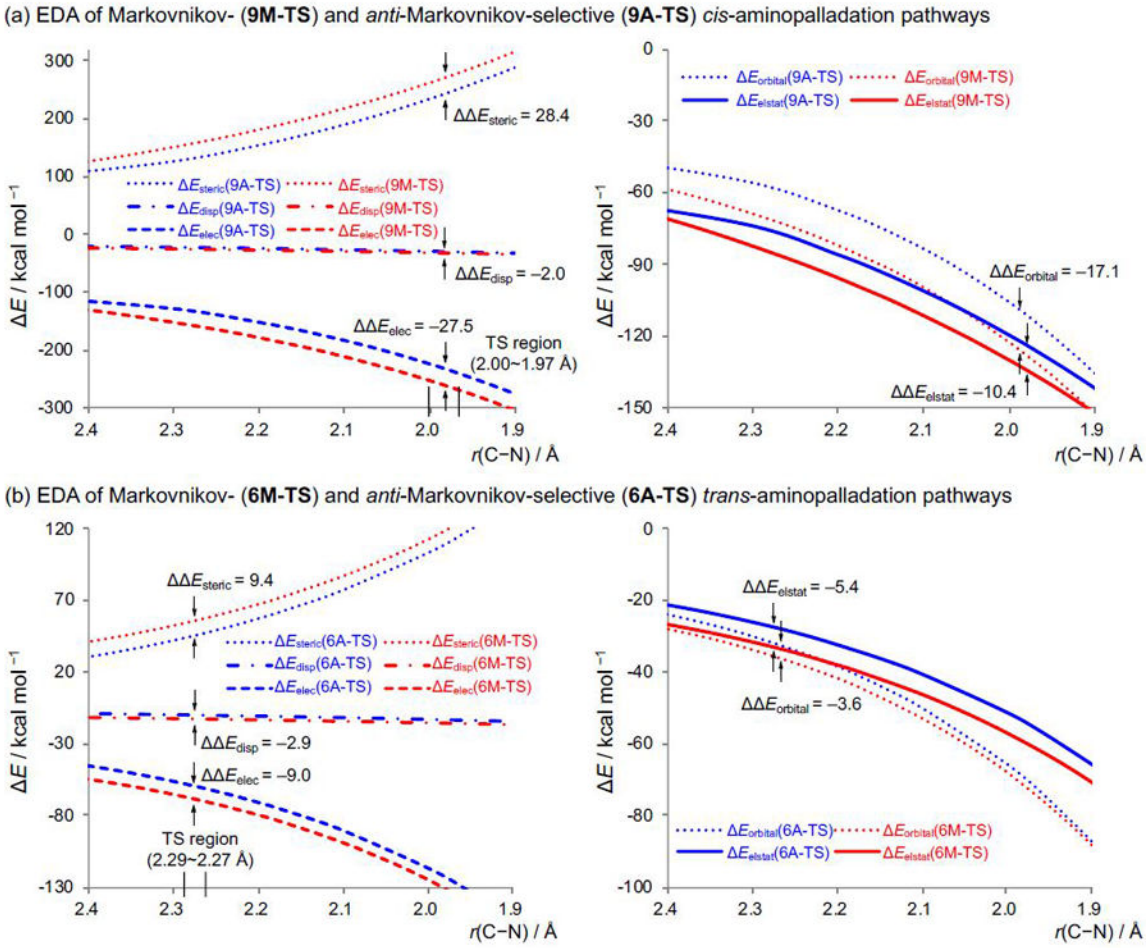

Figure 6.

Energy decomposition analysis (EDA) along the reaction coordinates of neutral Pd-catalyzed cis- and trans-aminopalladation (**a** and **b**, respectively) with phthalimide anion. The overall electronic effect term (ΔE_{elec}, left column) is further dissected into electrostatics (ΔE_{elstat}) and orbital interactions ($\Delta E_{orbital}$) in the right column. The DDE values are calculated from the energy difference between Markovnikov and anti-Markovnikov transition states (DDE = $DE_M - DE_A$). Therefore, positive DDE values indicate terms that favor anti-Markovnikov transition state; negative values indicate terms that favor Markovnikov transition state.

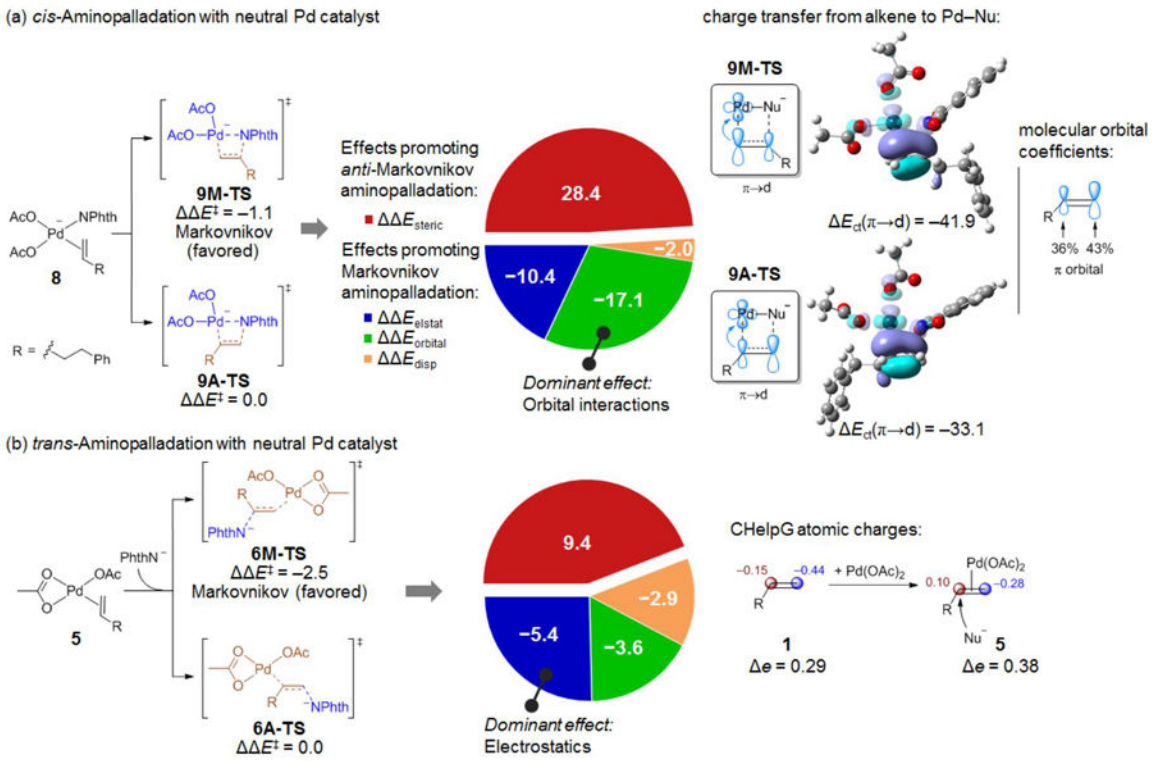

Figure 7.

Contributions of different types of nucleophile-substrate interactions to the regioselectivity in neutral $Pd(OAc)_2$-catalyzed cis- and trans-aminopalladation with phthalimide anion. The computed regioselectivity ($DDE_{‡}$) is calculated from the energy difference between Markovnikov and anti-Markovnikov transition states ($DDE_{‡} = DE_{M‡} – DE_{A‡}$). Each energy component (DDE_{steric}, DDE_{elstat}, $DDE_{orbital}$, and DDE_{disp}) is calculated in a similar fashion ($DDE = DE_M – DE_A$). Positive DDE values indicate effects that promote anti-Markovnikov addition; negative DDE values indicate effects that promote Markovnikov addition. All energies are in kcal/mol. The **π**→d charge transfer energies (DE_{ct}) in **9M-TS** and **9A-TS** were calculated using COVP analysis (the donor orbital is shown in solid; the acceptor orbital is shown in transparent). The molecular orbital coefficients of the C=C double bond in alkene **1** was calculated at B3LYP/6–31G(d) level.

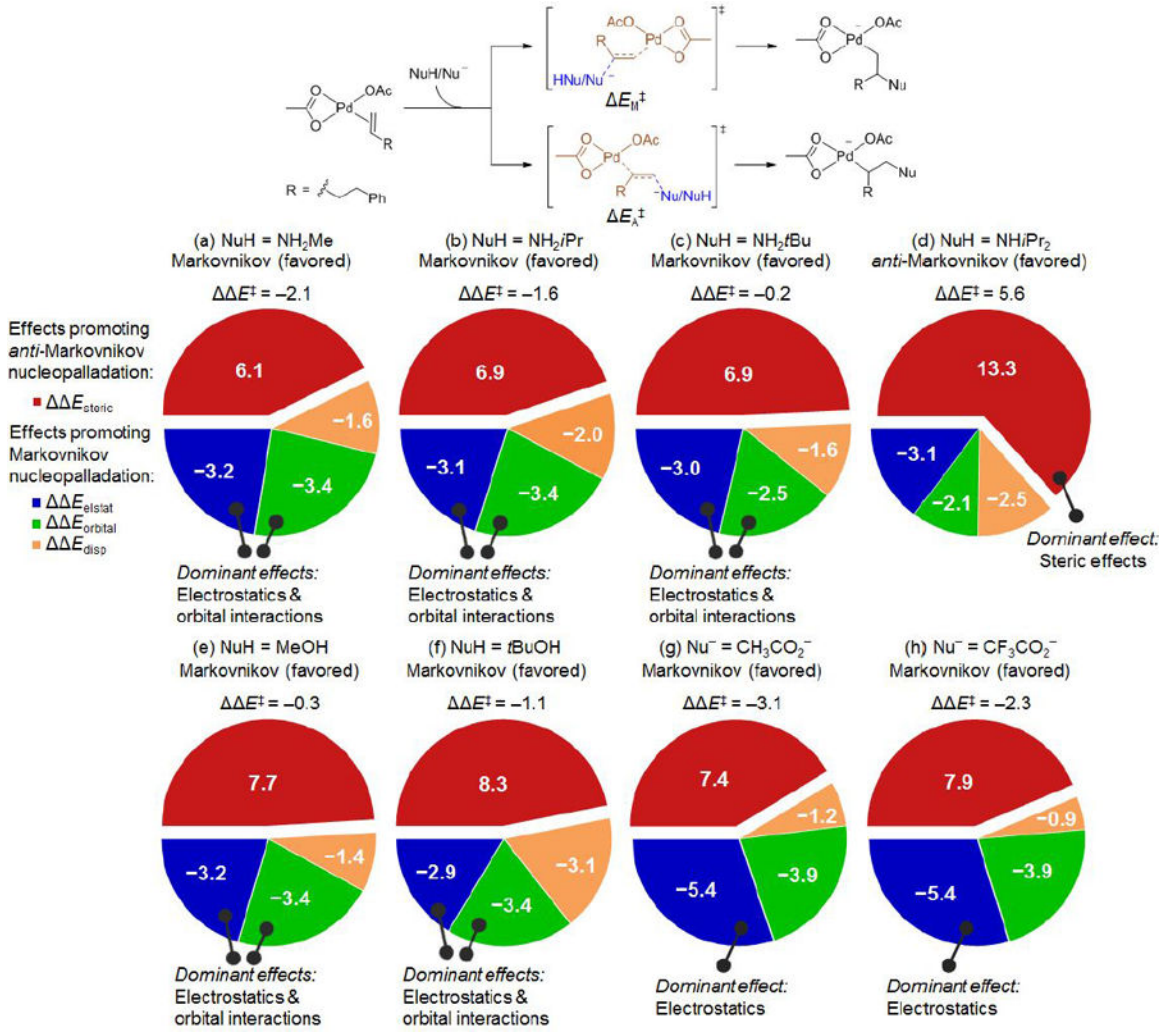

Figure 8.

Origins of regioselectivity in neutral $Pd(OAc)_2$-catalyzed trans-nucleopalladation with different N- and O-nucleophiles. The computed regioselectivity ($DDE_‡$) is calculated from the energy difference between Markovnikov and anti-Markovnikov transition states ($DDE_‡ = DE_{M‡} – DE_{A‡}$). Each energy component (DDE_{steric}, DDE_{elstat}, $DDE_{orbital}$, and DDE_{disp}) is calculated in a similar fashion ($DDE = DE_M – DE_A$). Positive DDE values indicate effects that promote anti-Markovnikov addition; negative DDE values indicate effects that promote Markovnikov addition. All energies are in kcal/mol.

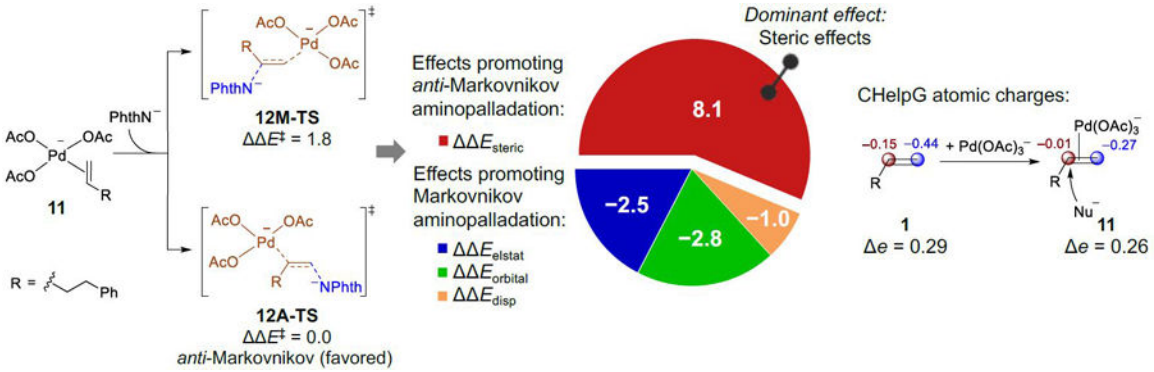

Figure 9.

Comparison of different types of nucleophile-substrate interactions on the regioselectivity in anionic palladate-catalyzed trans-aminopalladation with phthalimide anion. The computed regioselectivity ($DDE_{‡}$) is calculated from the energy difference between Markovnikov and anti-Markovnikov transition states ($DDE_{‡} = DE_{M‡} – DE_{A‡}$). Each energy component (DDE_{steric}, DDE_{elstat}, $DDE_{orbital}$, and DDE_{disp}) is calculated in a similar fashion ($DDE = DE_M – DE_A$). All energies are in kcal/mol.

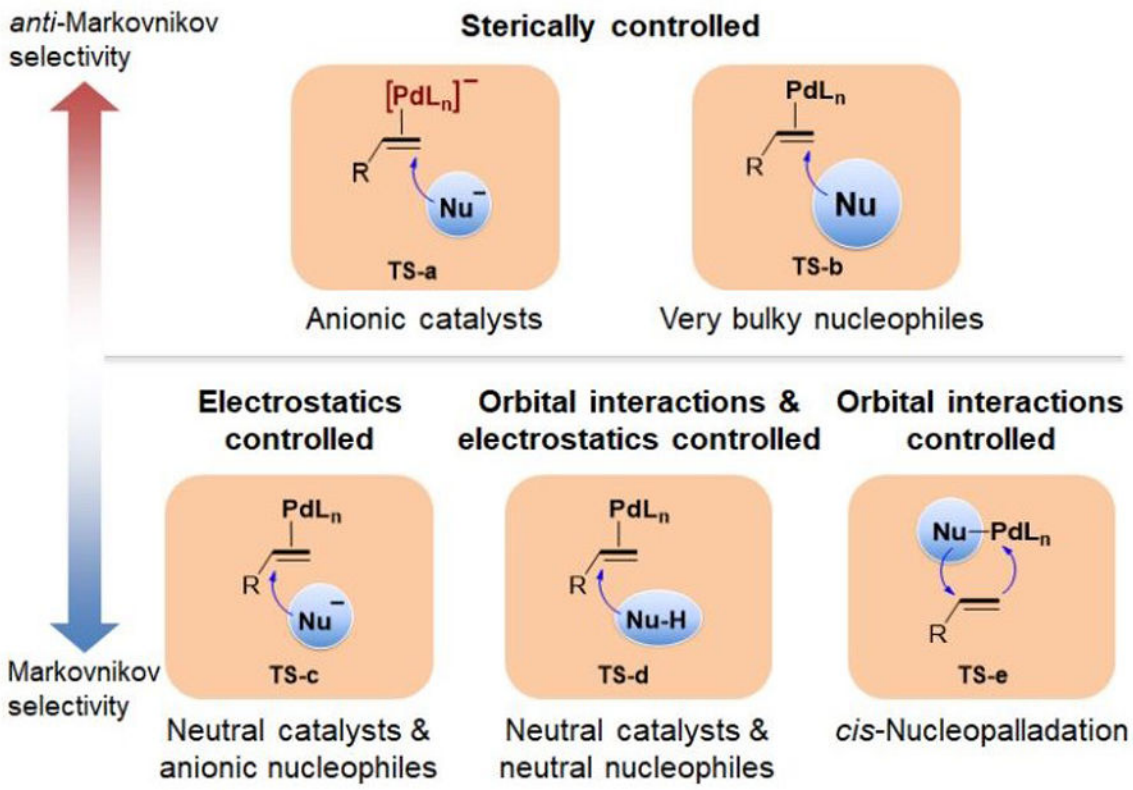

Figure 10.
Effects of catalyst and nucleophile on the dominant factor on regioselectivity.